CHALMERS
UNIVERSITY OF TECHNOLOGY

Real-Time Mixed-Integer Energy Management Strategy for Multi-Motor Electric Vehicles

Downloaded from: https://research.chalmers.se, 2025-12-05 04:39 UTC

Citation for the original published paper (version of record):

Ganesan, A., Murgovski, N., Yang, D. et al (2023). Real-Time Mixed-Integer Energy Management Strategy for Multi-Motor Electric Vehicles. 2023 IEEE Transportation Electrification Conference and Expo, ITEC 2023. http://dx.doi.org/10.1109/ITEC55900.2023.10186957

N.B. When citing this work, cite the original published paper.

© 2023 IEEE. Personal use of this material is permitted. Permission from IEEE must be obtained for all other uses, in any current or future media, including reprinting/republishing this material for advertising or promotional purposes, or reuse of any copyrighted component of this work in other works.

(article starts on next page)

Real-Time Mixed-Integer Energy Management Strategy for Multi-Motor Electric Vehicles

Anand Ganesan[†‡], Nikolce Murgovski[†], Derong Yang[‡] and Sebastien Gros[§]

***Abstract*—This paper[1] presents a real-time capable energy management strategy for multi-motor electric vehicles, based on mixed-integer model predictive control (MI-MPC). In this strategy, torque allocation and clutch on-off are co-optimized to minimize both the energy consumption and the frequent changes in clutch engagement status. To be able to solve the mixed-integer (MI) problem in real time, we propose a bi-level programming approach in which the torque allocation subproblem is solved at the inner level using an explicit closed-form analytical solution, while the integer decisions are optimized at the outer level using implicit dynamic programming (i-DP). The simulation results show that the proposed strategy can achieve up to $11\,\%$ energy savings, depending on the load demand in a driving mission, compared to a rule-based controller typically used in production vehicles. In addition, the proposed approach is guaranteed to find the global optimum for the MI problem in each MPC update. With a mean time to solution of around $4.6\,\mathrm{ms}$, the proposed strategy shows promising real-time capabilities for online implementation in multi-motor electric vehicles.**

I. Introduction

Although electric vehicles are a widely accepted solution to tackle climate change challenges [1], [2], a major factor that restricts the rate of mass adaptation is their driving range per charge [2]. An effective way to improve the range per charge of an electric vehicle (EV) is to maximize the operational efficiency of its powertrain.

In modern EV powertrains, a distributed architecture with multiple drivetrains is preferred due to its modularity and performance benefits over a single drivetrain unit [3]–[7]. In such multi-motor electric vehicles (MMEVs), decoupling mechanisms are also included to reduce idle losses, e.g., a clutch to isolate a drivetrain from its wheel(s) at zero torque demand [8], [9]. However, frequent changes in the engagement status of such mechanisms adversely affect key vehicle attributes like driveability, passenger comfort, component warranty, etc. [10]. Such distributed architectures offer two key categories of controls to optimize operational efficiency: $1)$ Distribution of driver demand among its electric drives and friction brakes, called control allocation [11], and $2)$ Decoupling decisions. Control allocation is further divided into distribution between front and rear wheels (or axles) [4], [12] and distribution between left and right wheels [7], [8]. In this paper, we focus on front-rear distribution and decoupling decisions.

Depending on the chosen control variable, the control allocation (CA) subproblem is also referred to as torque or power or force allocation (or split or distribution) in general [12]–[16]. Most of the energy management studies on MMEVs have focused solely on CA and ignored decoupling decisions. For example, the offline optimization (explicit) approaches proposed in [5], [6], [14] find numerical solutions (like optimal distribution maps), while those in [7], [12] derive analytical solutions for CA. A few studies have investigated the benefits of considering the decoupling decisions along with CA. For example, clutch on-off decision was optimized offline along with torque distribution in [8], while an online heuristic search was proposed for the clutch decision in [4]. Although these approaches showed increased energy savings compared to optimizing CA alone, the main drawbacks of these approaches are, $1)$ suboptimal solutions and $ii)$ instantaneous clutch decisions. Such decisions result in frequent changes in clutch engagement (discussed in Section V-D1) that adversely affect comfort, warranty, etc. Therefore, an energy management strategy that considers the cost of clutch transitions while optimizing both CA (continuous) and clutch on-off (integer) decisions is needed and has yet to be proposed for MMEVs.

In addition, optimizing both control decisions results in a mixed-integer (MI) problem that is generally NP-hard due to the combinatorial nature of integer decisions. NP stands for 'nondeterministic polynomial time' and refers to a complexity class of problems that can be solved in polynomial time, e.g., the CA problem, while NP-hard are at least as hard as the hardest problems in NP [17]. An algorithm that guarantees to find global solution to such an MI problem suffers from exponential worst-case time complexity [17]. For example, Dynamic Programming (DP) and direct methods like branch-and-bound, cutting planes, etc., [18]–[20] are widely used to find global solutions to such MI problems offline. However, these methods are computationally too expensive to implement in real time due to the combinatorial nature of the problem and suffer from large run-time variations. Therefore, computationally efficient solutions that overcome these challenges are vital for online implementation of MI strategies in MMEVs.

In this work, we first propose a mixed-integer model predictive control based energy management strategy that co-optimizes both front-rear torque distribution and clutch on-off decisions online, to improve operational efficiency of an MMEV. In this strategy, we penalize frequent changes in clutch engagement status using a clutch dynamics model and a

[1]This work was supported by the *Sweden's Innovation Agency (Vinnova)* under Grant 2017-05506.

[†]Dept. of Electrical Engineering, Chalmers University of Technology, Göteborg, Sweden. {anandg,nikolce.murgovski}@chalmers.se

[‡]Dept. of Software Engineering, R&D, Volvo Cars, Göteborg, Sweden. {anand.ganesan,derong.yang}@volvocars.com

[§]Dept. of Engineering Cybernetics, Norwegian University of Science and Technology, Trondheim, Norway. sebastien.gros@ntnu.no

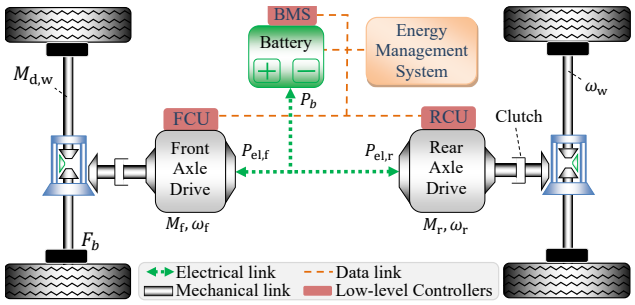

Fig. 1: Simplified representation of a multi-motor electric vehicle powertrain consisting of two electric drives and a battery. The Energy Management System block hosts the proposed controller and sends optimal references to the lower-level controllers. BMS refers to battery management system.

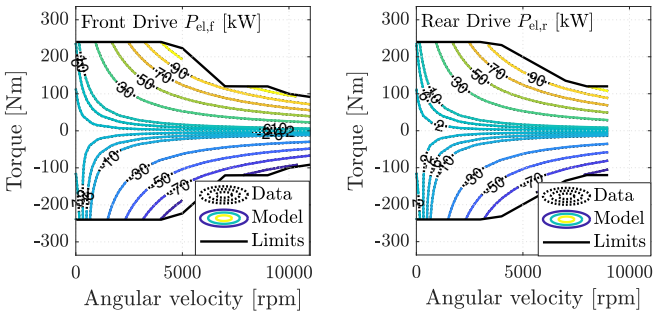

Fig. 2: Contour plots comparing model estimates (solid line) and measured (dotted line) power consumption for front and rear EDs when $x = \mathbf{1}$.

tunable transition cost while minimizing the energy consumption of the EV. Second, we propose a bi-level programming approach to solve the resulting MI problem in real-time, efficiently and optimally. In this approach, the CA subproblem is solved at the inner level using an explicit closed-form analytical solution, while the clutch decisions are optimized at the outer level using implicit dynamic programming (i-DP).

II. Control Model of BEV Powertrain

This section describes the control-oriented modeling of the multi-motor battery electric vehicle (BEV) powertrain shown in Fig. 1. The front control unit (FCU) and rear control unit (RCU) control the electric drive (ED) and driveline clutch of the front and rear axles, respectively.

A. Modeling Clutch Dynamics and its Transition Cost

Clutches in an EV powertrain can be used to reduce idle losses by isolating the drivetrain(s) from the wheels. Subsequently, the steady-state conditions, (referred to as engagement status) of a dry clutch, are modeled as either engaged (on $\Leftrightarrow 1$) or disengaged (off $\Leftrightarrow 0$). Let $x = [x_\mathrm{f}\ x_\mathrm{r}]^T$ and $u_\mathrm{c} = [u_\mathrm{f}\ u_\mathrm{r}]^T$ denote the state and control vectors of the clutch dynamics model. The subscripts f and r are used to represent front and rear axles, respectively. The engagement status of the clutches is then modeled as discrete states with integer controls as

$$x(k+1) := x(k) + u_\mathrm{c}(k), \qquad \forall k, \quad (1)$$

$$x(k) \in \mathbb{B} \subseteq \{0,1\}^2,\ u_\mathrm{c}(k) \in \mathcal{U}_\mathrm{c} \subseteq \{-1,0,1\}^2, \quad \forall k, \quad (2)$$

where k is the discrete-time instance, $\mathbb{B}$ and $\mathcal{U}_\mathrm{c}$ denote the feasible and admissible sets for the state and control vectors.

The transient dynamics of the clutch (slipping phases) is not explicit in model (1). However, a non-zero control (i.e., $u_i \neq 0$) represents an instance of clutch transition in the i^{th} axle where $i \in \{\mathrm{f},\mathrm{r}\}$. Subsequently, the power loss during these clutch transitions $P_{\mathrm{c},i}$ is modeled as a discrete cost function whose value is non-zero only at instances of change, i.e.,

$$P_{\mathrm{c},i}(k) := \begin{cases} 0, & u_i(k) = 0, \quad \forall k,\ i \in \{\mathrm{f},\mathrm{r}\} \\ b_{\mathrm{c},i}\|u_i\|, & u_i(k) \neq 0, \quad \forall k,\ i \in \{\mathrm{f},\mathrm{r}\} \end{cases} \quad (3)$$

where $b_{\mathrm{c},i} \in \mathbb{R}_+$ represents the unit power loss for a single clutch transition on the i^{th} axle. Therefore, the total cost due to the transition of both clutches is defined as $P_\mathrm{c} = P_{\mathrm{c},f} + P_{\mathrm{c},r}$.

B. Electrical Power Consumption of the BEV Powertrain

Each ED comprises an electric machine (EM), an inverter, and a fixed ratio transmission. The losses in these components, i.e., total losses in an ED ($P_{\mathrm{ls},i} \in \mathbb{R}_{\geq 0}$) and subsequently, the power consumption of an ED ($P_{\mathrm{el},i}$), are approximated as a quadratic polynomial of its EM torque ($M_i \in \mathbb{R}$) as

$$P_{\mathrm{el},i} := f_1(M_i, \omega_i, x_i) \approx P_{\mathrm{ls},i} + \omega_i M_i,\ \ i \in \{\mathrm{f},\mathrm{r}\}, \quad (4)$$

$$P_{\mathrm{ls},i} := f_2(M_i, \omega_i, x_i) \approx x_i b_{i0}(\omega_i) + \sum_{j=1}^{2} b_{ij}(\omega_i)|M_i|^{(j)}. \quad (5)$$

The bounds on the EM torque depend on the angular velocity of the EM ($\omega_i(k)$) and the clutch status on i^{th} axle, i.e.,

$$\underline{c}_i(\omega_i, k)x_i(k) \leq M_\mathrm{i}(k) \leq \bar{c}_i(\omega_i, k)x_i(k), \qquad \forall k,\ \forall i, \quad (6)$$

where the velocity-dependent torque limits $\underline{c}_i, \bar{c}_i$ include the power limitations of the EM at high speeds. This model has a mean absolute percentage error of around 2 % (refer Fig. 2).

C. Vehicle Dynamics and Torque Demand Estimation

This study focuses on the front-rear torque distribution and therefore, we consider only the longitudinal vehicle dynamics and assume linear operation of tires. Subsequently, we ignore the effect of load transfer, and wheel and tire slip losses. Furthermore, we assume that vehicle speed v and road slope α are perfectly known a priori as optimizing v is not a focus. Then, the traction force demand for the mission is given by

$$\begin{aligned} F_\mathrm{t}(k) =& a(k)m_\mathrm{e}(x,k) + c_\mathrm{d}A_\mathrm{f}\rho_\mathrm{a}v^2(k)/2 + F_\mathrm{b}(k) \\ &+ mg\left(\sin\alpha(k) + c_\mathrm{r}\cos\alpha(k)\right), \end{aligned} \quad (7)$$

where a denotes acceleration, c_d and c_r refer to air and rolling resistance coefficients, A_f refers to frontal area, ρ_a refers to air density, m refers to vehicle mass, and F_b is the force dissipated in friction brakes. The equivalent mass is stated as

$$m_\mathrm{e}(k) = m + \left(\left(J_\mathrm{w} + x_\mathrm{f}(k)J_\mathrm{f}R_\mathrm{f}^2 + x_\mathrm{r}(k)J_\mathrm{r}R_\mathrm{r}^2\right)/r_\mathrm{w}^2\right), \quad (8)$$

where r_w refers to wheel radius, $R_{(\cdot)}$ and $J_{(\cdot)}$ refer to the fixed transmission ratio and the inertia of ED in an axle, and J_w denotes the inertia of wheels and driveline components. Given that the brake control unit (BCU) always ensures that

$$F_\mathrm{b}(k) = \begin{cases} 0, & F_\mathrm{t}(k) > \underline{F}_{\mathrm{rg,pt}}(k), \\ F_\mathrm{t}(k) - \underline{F}_{\mathrm{rg,pt}}(k), & \text{otherwise}, \end{cases} \quad (9)$$

the wheel torque demand (M_d), and the velocities of the wheel (ω_w) and the ED ($\omega_i,\ \forall i$) are calculated a priori as

$$M_\mathrm{d}(k) = \max\left(F_\mathrm{t}(k), \underline{F}_{\mathrm{rg,pt}}(k)\right) r_\mathrm{w}, \tag{10}$$

$$\underline{F}_{\mathrm{rg,pt}}(k) = \underline{F}_{\mathrm{rg,f}}(v, x_\mathrm{f}, k) + \underline{F}_{\mathrm{rg,r}}(v, x_\mathrm{r}, k)), \tag{11}$$

$$\omega_\mathrm{w}(k) = v(k)/r_\mathrm{w},\ \omega_i(k) = x_\mathrm{i}(k)\omega_\mathrm{w}(k)R_i,\ \forall i. \tag{12}$$

where $\underline{F}_{\mathrm{rg,pt}}, \underline{F}_{\mathrm{rg,f}}, \underline{F}_{\mathrm{rg,r}} \in \mathbb{R}_-$ denote the regeneration limits of the powertrain and the EDs, respectively. The prior estimation of the terms $m_\mathrm{e},\ \underline{F}_{\mathrm{rg},i}$ and ω_i for all i is made conservative by deriving the cumulative load under closed clutches ($x = 1$). This overestimates m_e, but the effect is negligible since $J_\mathrm{f}, J_\mathrm{r} \ll m r_\mathrm{w}^2/R_{(\cdot)}^2$.

III. MI Energy Management Problem

A. Control Architecture and the Proposed Controller

We use a hierarchical three-layer control framework similar to that in [21, Fig. 4]. At the top level, an oracle optimizes v and battery state of energy (x_b) for the entire mission based on route and traffic predictions from cloud-based navigation services. The bottom level controllers transmit the current-state estimates to the upper levels. In the middle layer, the supervisory co-optimization controller (SCC) that hosts the proposed energy management strategy uses this information to optimize the MI decisions and minimize energy consumption.

B. Mixed-Integer MPC (MI-MPC) Problem Formulation

The goal of the energy management problem is to deliver the wheel torque demand at each instant using the five controls $u = [u_\mathrm{f}\ u_\mathrm{r}\ M_\mathrm{f}\ M_\mathrm{r}\ M_\mathrm{b}]^T$ so that both the energy consumption of the powertrain and the frequent changes in the clutch engagement status are minimized, while adhering to the clutch dynamics (x). Among these controls, the torque allocated to the friction brakes M_b^* is already factorized in (10) using (9) which minimizes the energy lost in braking. Therefore, the demand (10) must be met by the remaining actuators. This leads to a demand balance constraint as, $R_\mathrm{f}M_\mathrm{f} + R_\mathrm{r}M_\mathrm{r} = M_\mathrm{d}$. Note that this constraint is implicitly affected by state x via the torque bounds in (6). Then, a variable substitution as $M_\mathrm{r} = (M_\mathrm{d} - M_\mathrm{f}R_\mathrm{f})/R_\mathrm{r}$ simplifies the control vector as $\tilde{u} = [u_\mathrm{f}\ u_\mathrm{r}\ M_\mathrm{f}]^T$ and the EM torque limits in (6). Then, from (4), the rate of powertrain energy consumption is defined as

$$\begin{aligned} P_\mathrm{b}(k) = {} & P_{\mathrm{ls,f}}(x_\mathrm{f}, k) + x_\mathrm{r}(k)M_\mathrm{d}(k)\omega_\mathrm{w}(k) \\ & + P_{\mathrm{ls,r}}(x_\mathrm{r}, k) + (x_\mathrm{f}(k) - x_\mathrm{r}(k))\omega_\mathrm{w}(k)R_\mathrm{f}M_\mathrm{f}(k). \end{aligned} \tag{13}$$

Finally, the MI-MPC implementation of the energy management problem to be solved online by the SCC is,

$$\min_{x,\tilde{u}} \quad \sum_{k=1}^{N} \phi\left(x, \tilde{u}, \theta, k\right)\ \Delta t \tag{14a}$$

$$\text{s.t} \quad (1) \text{ and } (2), \tag{14b}$$

$$\underline{c}(x, \theta, k) \le \mathbf{1}M_\mathrm{f}(k) \le \overline{c}(x, \theta, k), \qquad \forall k, \tag{14c}$$

where index $(k) \mapsto (k|j)$, $k \in \{1, 2, ..., N\}$ denotes time step, $j \in \{1, 2, ..., (t_\mathrm{f}/\Delta t) - N\}$ refers to the MPC instance, Δt is the sampling interval, θ refers to the parameter vector, and $t_\mathrm{f}, N \in \mathbb{Z}_{>0}$ refers to the final time and prediction window, respectively. The stage cost (ϕ) and the bounds ($\overline{c}, \underline{c}$) are

$$\phi := P_\mathrm{b}\left(x, M_\mathrm{f}, \theta, k\right) + P_\mathrm{c}\left(u_\mathrm{c}, \theta, k\right), \tag{15}$$

$$\underline{c} := [\ \underline{c}_\mathrm{f}(k)x_\mathrm{f}(k), \quad (M_\mathrm{d}(k) - x_\mathrm{r}(k)\overline{c}_\mathrm{r}(k)R_\mathrm{r})/R_\mathrm{f}\ ]^T, \tag{16}$$

$$\overline{c} := [\ \overline{c}_\mathrm{f}(k)x_\mathrm{f}(k), \quad (M_\mathrm{d}(k) - x_\mathrm{r}(k)\overline{c}_\mathrm{r}(k)R_\mathrm{r})/R_\mathrm{f}\ ]^T. \tag{17}$$

IV. Solving the Mixed-Integer Problem

In this section, we describe the proposed bi-level programming approach to solve the MI-MPC problem (14) online. In this approach, the torque allocation subproblem is solved at the inner level, while integer decisions are optimized at the outer level using implicit dynamic programming (i-DP).

A. Closed-Form Analytical Solution for the CA Subproblem

When the clutch engagement status x is known, the problem (14) simplifies to a static optimization problem at each k as

$$\min_{M_\mathrm{f}} \left\{ \left(P_\mathrm{b}(x, M_\mathrm{f}, \theta, k)\right) \ \middle|\ \underline{M}(k) \le M_\mathrm{f}(k) \le \overline{M}(k) \right\}, \tag{18}$$

where $\underline{M} = \max\left(\underline{c}(x, \theta, k)\right)$ and $\overline{M} = \min\left(\overline{c}(x, \theta, k)\right)$. Notice that the term $(x_\mathrm{f} - x_\mathrm{r})\omega_\mathrm{w}R_\mathrm{f}M_\mathrm{f}$ in (13) becomes 0 in all-wheel-drive mode ($x = \mathbf{1}$). This simplifies the problem (18) to a static power loss minimization problem whose cost function is quadratic over the variable M_f (based on the models in (5)). Then, its closed-form analytical solution is derived as

$$\hat{M}_\mathrm{f}^* := \begin{cases} \overline{M}(k), & \hat{M}_\mathrm{f}^{\mathrm{ub}}(\cdot) \ge \overline{M}(k), \\ \underline{M}(k), & \hat{M}_\mathrm{f}^{\mathrm{ub}}(\cdot) \le \underline{M}(k), \\ \hat{M}_\mathrm{f}^{\mathrm{ub}}(x, \theta, k), & \text{otherwise}, \end{cases} \tag{19}$$

$$\hat{M}_\mathrm{f}^{\mathrm{ub}} := \begin{cases} \frac{(b_{\mathrm{r}1}R_\mathrm{f}R_\mathrm{r} - b_{\mathrm{f}1}R_\mathrm{r}^2 + 2\,b_{\mathrm{r}2}R_\mathrm{f}\,|M_\mathrm{d}|(k))\mathrm{sgn}(M_\mathrm{d})}{2\,b_{\mathrm{f}2}R_\mathrm{f}^2 + 2\,b_{\mathrm{r}2}R_\mathrm{r}^2}, & x = \mathbf{1}, \\ x_\mathrm{f}\ M_\mathrm{d}(k)/R_\mathrm{f}, & x \ne \mathbf{1}, \end{cases}$$

where $\hat{M}_\mathrm{f}^*$ and $\hat{M}_\mathrm{f}^{\mathrm{ub}}$ denote optimal and unbounded policies, respectively. For powertrains with identical ED on both axles, the solution simplifies to $\hat{M}_\mathrm{f}^{\mathrm{ub}} = 0.5\,M_\mathrm{d}/R_\mathrm{f}$ for $x = \mathbf{1}$.

B. Solving the Clutch On-Off Decisions at the Outer Level

A bi-level formulation of the MI problem (14) is stated as

$$[x^*(k), \tilde{u}^*(k)] = \arg\min_{x,\tilde{u}} \quad \sum_{k=1}^{N} \phi\left(x, \tilde{u}, \theta, k\right)\ \Delta t \tag{20a}$$

$$\text{s.t} \quad (1) \text{ and } (2), \tag{20b}$$

$$x_\mathrm{f}(k) + x_\mathrm{r}(k) \ge p(k), \tag{20c}$$

$$M_\mathrm{f}(k) \in \hat{M}_\mathrm{f}^*(x, k). \tag{20d}$$

where, $p = \{0\ |M_\mathrm{d}(k) = 0\}$ and $p = \{1\ |M_\mathrm{d}(k) \ne 0\}$. The constraint (20c) ensures that at least a clutch is closed if $M_\mathrm{d} \ne 0$. This bi-level problem is solved in real time using the i-DP method. Note that the constraint (20d) denotes the optimal policy (19) of the torque allocation subproblem (18). Consequently, i-DP optimizes clutch on-off decisions online based on the policy (19). This proposed bi-level approach has two key benefits: 1) The i-DP guarantees a global optimum for the MI problem (14) since the policy (19) provides an exact

TABLE I: Parameters used in the simulation study

Parameter	Value	Parameter	Value
A_f	1.92 m^2	J_w	2.5 kgm^2
c_d	0.019	$J_\mathrm{f} = J_\mathrm{r}$	0.06 kgm^2
c_r	0.01	R_f	10
m	1800 kg	R_r	8
g	9.82 m/s^2	$b_{\mathrm{c,f}} = b_{\mathrm{c,r}}$	0.10 kW
ρ_a	1.18 kg/m^3	Δt , t_h	1 s, 5 s
r_w	0.37 m	EM Max Torque	$\approx$ 230 Nm
Top Speed	160 km/h	ED Peak Power	$\approx$ 120 kW (Front)
EM Type	PMSM		$\approx$ 110 kW (Rear)

TABLE II: Test cycles used to evaluate the performance of proposed strategy

Scenarios	Driving / Test Cycle	Acronym
City/Urban Driving	Gothenburg City Cycle [8]	GCC
	Common Artemis Driving Cycle (CADC) urban	C-Urbn
Mixed Driving	Worldwide Harmonised Light Vehicles Test Procedure	WLTC
	Common Artemis Driving Cycle (CADC) Rural	C-Rurl
Highway Driving	US06 supplemental federal test procedure (SFTP)	US06
	Common Artemis Driving Cycle (CADC) Motorway150	C-Hway

optimum for the continuous decision variable (M_f^*) which enables to avoid the loss in optimality typically associated with the need to discretize such variables in DP. 2) The online computational demand is significantly reduced as i-DP searches only over the two binary variables instead of the decision space of the three variables.

V. Simulation Results and Discussion

This section describes the simulation setup and the evaluation results of the proposed MI energy management strategy and the solution strategy based on bi-level programming.

A. Simulation Setup and Reference Controller

To validate the proposed strategies, we perform a dynamic simulation using the plant models of the BEV powertrain. The only difference between the plant and control models is the approximation of m_e in the latter, as stated in Section II-C. A feedback mechanism is used to compensate for speed deviations arising from this modeling uncertainty. Furthermore, we assume a perfect prediction of v and α to estimate demand trajectories, as prediction uncertainties are not the focus in this work. The model and simulation parameters are provided in Table I. Since, we consider only the discrete clutch dynamics the chosen horizon covers 4 future states which was found to be sufficient for this study. The control and prediction horizons are kept the same for simplicity.

Table II shows the six driving profiles used to evaluate performance under three different driving scenarios. In addition, a rule-based controller typically used in production vehicles was simulated for comparison and is referred to as equal torque distribution (ETD). The heuristic rules used by ETD to decide clutch on-off and torque allocation decisions are expressed as

$$x_\mathrm{i} := \begin{cases} 0, & M_\mathrm{i} = 0, \ \forall i, \\ 1, & \text{otherwise}, \ \forall i, \end{cases} \tag{21}$$

$$M_i := \max(\underline{c}_i, \ \min(\bar{c}_i, \ 0.5 M_\mathrm{d}/R_i)), \quad \forall i. \tag{22}$$

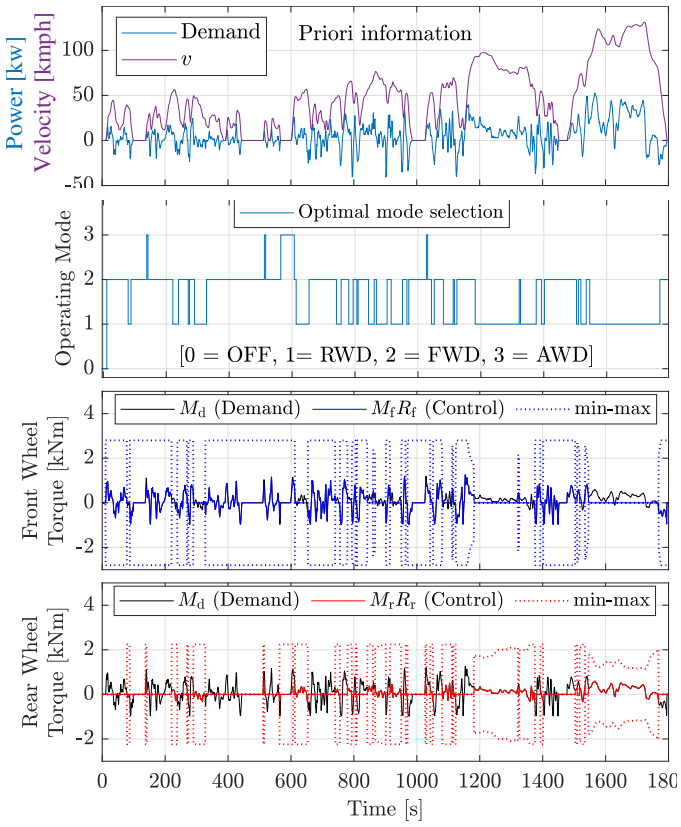

Fig. 3: Optimal trajectories of proposed MI strategy for WLTC. The mode is post processed based on Table III. The states and controls are within bounds.

TABLE III: Relation between operating mode and clutch engagement status

Operating Mode	Mode Number	Front Clutch Status (x_f)	Rear Clutch Status (x_r)
Powertrain Disabled (OFF)	0	0	0
Rear Wheel Drive (RWD)	1	0	1
Front Wheel Drive (FWD)	2	1	0
All Wheel Drive (AWD)	3	1	1

B. MI Optimal Solution of the Proposed Strategy

Fig. 3 shows the solution trajectories of the proposed MI strategy for the WLTC Class-3b. The wheel torque subplots denote the front-rear torque distribution w.r.t. the demand M_d. Operating mode subplot shows that FWD or RWD is chosen mostly, whereas AWD is chosen only at a few points. Such mode choices were found to depend on the policy (19), M_d, v and the chosen $b_{\mathrm{c},i}$. We will analyze how these factors influence mode selection in our future work. Also, note that the OFF mode ($x = \mathbf{0}$) is not chosen during the mission (except at the start), i.e., at least one clutch remains engaged, as there are no losses in EDs when both the speed (v) and torque demand (M_d) are zero. Furthermore, the front wheel torque limits are higher than the rear wheel limits, as the front ED has a higher ratio than that at the rear, as stated in Table I. In addition, note that x also affects torque limits as stated in (6).

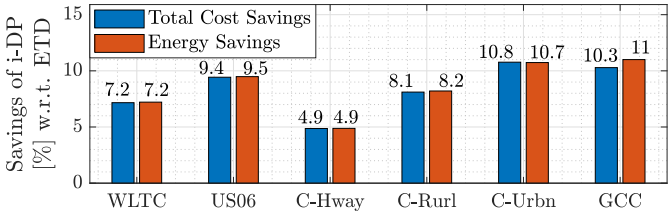

(a) The proposed i-DP based MI strategy consistently realizes significant cost and energy savings across the driving missions. The contribution of clutch changes in the total cost depends on the chosen penalty $b_{c,i}$. The total cost of ETD is post processed based on (15).

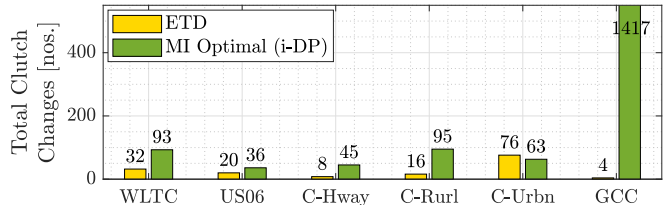

(b) The MI strategy shows significant increase of over 100 % in total clutch changes in almost all cycles, with the worst performance observed in GCC.

Fig. 4: Comparison of the total cost and its principal components (energy consumption and total clutch transitions) for the proposed MI strategy w.r.t. the values of the ETD strategy, for the chosen penalty of 0.1 kW. The proposed strategy compromises on clutch transitions to achieve significant energy and total cost savings across driving missions.

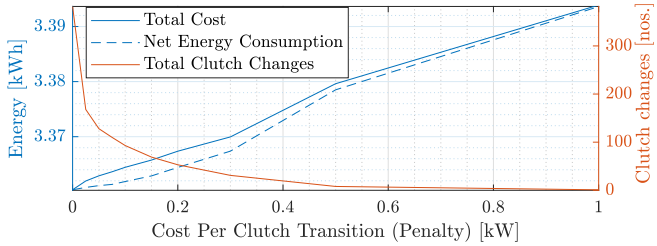

(a) Effect of the choice of clutch penalty on the total cost and its two sub costs: consumption and clutch transitions, for WTLC. The total cost always increases with the penalty. However, zero penalty minimizes energy consumption but maximizes clutch transitions and vice-versa. Notice that the penalty of optimal balance, chosen in Fig. 5(b), almost corresponds to the intersection of the two sub costs in this plot. This observation of chosen penalty is consistent across all the missions.

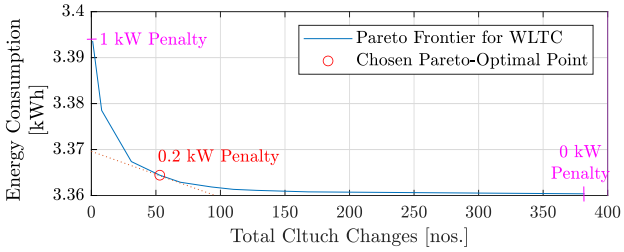

(b) This figure shows the Pareto front of the conflicting objectives for WLTC. To find an optimal balance of the two costs, we choose the point that is closest to the origin, i.e., the utopia point of the frontier. Subsequently, the penalty that corresponds to this chosen point is 0.2 kW which is shown in the figure.

Fig. 5: This figure shows the effect of the choice of cost per clutch transition (penalty) on the competing objectives for WTLC. Based on the Pareto front, we choose 0.2 kW as the penalty to optimally balance both energy consumption and clutch transitions.

C. Energy Savings Against No. of Clutch Transitions

The comparison of the total cost and its two principal components (energy consumption and total clutch transitions) of the strategies, in Fig. 4, shows that the proposed i-DP based MI strategy consistently realizes the best cost and energy savings across different driving missions. However, the controllers show an opposite trend for total clutch changes, where ETD performs the best. The results in Fig. 4 yield two important findings. 1) The MI strategy can lead to significant savings, but at the cost of increased clutch transitions for the chosen $b_{c,i}$. Achieving a balance between these two conflicting factors depends on their relationship and is therefore further analyzed in Section V-D1. 2) The effectiveness of the MI strategy in achieving energy savings depends on the severity of the missions parameters such as the load demand and speed.

D. Sensitivity and Computation Demand of Proposed Strategy

1) Effect of Clutch Transition Penalty on Competing Objectives: As the results in Fig. 4 revealed that energy consumption and the number of clutch transitions are indeed conflicting objectives, the proposed MI energy management strategy leads to a multi-objective (or Pareto) optimization problem.

Fig. 5(a) shows the sensitivity of the two conflicting objectives w.r.t. the choice of the cost per clutch transition (penalty) $b_{c,i}, \forall i$, for WTLC. It can be seen that the total cost always increases as the penalty increases. However, minimal energy consumption requires zero penalty, but maximizes clutch transitions. Such high transitions with zero penalty are expected since the MI problem (14) reduces to a static optimization problem and clutch decisions become instantaneous with zero penalty, as clutch dynamics (1) and transition cost (3) become irrelevant. Such high transitions adversely affect passenger comfort, warranty, etc. [10] and are therefore not preferred. (Notice that this reduced static problem is similar to the static problem solved offline in [8] and the instantaneous online heuristics in [4]. Hence, these strategies suffer from such high transitions and their effects.)

In contrast, Fig. 5(a) also shows that the clutch transitions decrease with a sufficiently high penalty, but energy consumption increases. Note that the choice of a high penalty of 1 kW results in a controller that operates purely in AWD mode in all cases and may lead to higher consumption than the ETD.

To avoid such extremes, we use the Pareto frontier of the costs shown in Fig. 5(b) to choose a penalty that balances the costs for WLTC. All points in the frontier are Pareto-optimal. But the penalty of 0.2 kW corresponds to the closest point to the origin (the utopian point of this frontier) [22] that optimally balances the costs. This analysis shows that the cost per clutch transition can be adjusted to achieve a balance between energy savings and comfort.

2) Computational Demand of the Proposed Strategies: All simulations in the study were performed in matlab environment on a computer with 32 GB of RAM and an octa-core processor operating at 2.3 GHz. The proposed MI solution strategy performs well in terms of computational efficiency

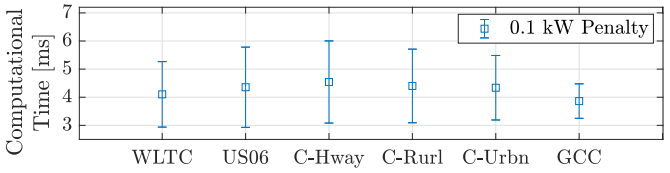

Fig. 6: Computational time statistics for a prototype implementation of the proposed bi-level approach based MI solution strategy. Mean computation time is less than 4.6 ms. Worst-case time is less than 6 ms.

with a mean and worst-case time of less than $4.6\,\mathrm{ms}$ and $6\,\mathrm{ms}$, respectively, in all missions considered. These results should be seen as a proof-of-concept, as they are based only on a prototype implementation of the DP method used in the proposed solution strategy. Subsequently, the order of magnitude of runtimes in Fig. 6 depicts pessimistic upper bounds for the algorithms, since further improvements are possible with software tailored for real-time MPC implementation. However, the actual runtime of an embedded EV onboard depends on its processing and memory capacities.

VI. Conclusion

A computationally efficient energy management strategy is proposed that co-optimizes control allocation and clutch on-off decisions online based on mixed-integer model predictive control for a multi-motor EV. The proposed strategy shows significant cost and energy savings of up to $11\,\%$ compared to a rule-based controller typically used in production vehicles. These savings vary depending on the severity of load demand in driving missions. However, these savings come at the cost of increased clutch transitions. The Pareto analysis shows that the cost per transition can be adjusted to achieve a balance between energy savings and comfort.

With a mean time to solution of around $4.5\,\mathrm{ms}$ and a worst-case time of less than $6\,\mathrm{ms}$, the proposed bi-level approach that is guaranteed to find the global solution to the MI energy management problem shows promising performance and real-time capabilities for online implementation in multi-motor electric vehicles.

References

[1] M. F. Felgenhauer, M. A. Pellow, S. M. Benson, and T. Hamacher, "Evaluating co-benefits of battery and fuel cell vehicles in a community in California," *Energy*, vol. 114, pp. 360–368, Nov. 2016.

[2] IEA (2021), "Global EV Outlook 2021," tech. rep., IEA, Paris. https://www.iea.org/reports/global-ev-outlook-2021.

[3] O. Nezamuddin, R. Bagwe, and E. Dos Santos, "A Multi-Motor Architecture for Electric Vehicles," in *2019 IEEE Transportation Electrification Conference and Expo (ITEC)*, pp. 1–6, June 2019.

[4] X. Yuan and J. Wang, "Torque Distribution Strategy for a Front- and Rear-Wheel-Driven Electric Vehicle," *IEEE Transactions on Vehicular Technology*, vol. 61, pp. 3365–3374, Oct. 2012.

[5] M. V. Castro, S. Mukundan, C. L. Filho, G. Byczynski, B. Minaker, J. Tjong, and N. Kar, "Non–Dominated Sorting Genetic Algorithm Based Determination of Optimal Torque–Split Ratio for a Dual–Motor Electric Vehicle," in *IECON 2021 – 47th Annual Conference of the IEEE Industrial Electronics Society*, pp. 1–6, Oct. 2021.

[6] S. De Pinto, P. Camocardi, C. Chatzikomis, A. Sorniotti, F. Bottiglione, G. Mantriota, and P. Perlo, "On the Comparison of 2- and 4-Wheel-Drive Electric Vehicle Layouts with Central Motors and Single- and 2-Speed Transmission Systems," *Energies*, vol. 13, p. 3328, June 2020.

[7] G. De Filippis, B. Lenzo, A. Sorniotti, P. Gruber, and W. De Nijs, "Energy-Efficient Torque-Vectoring Control of Electric Vehicles With Multiple Drivetrains," *IEEE Transactions on Vehicular Technology*, vol. 67, pp. 4702–4715, June 2018.

[8] J. Torinsson, *Power loss minimization in electric cars by wheel force allocation*. Licentiate Thesis, Chalmers University of Technology, Göteorg, Nov. 2020.

[9] R. Camilleri, P. Armstrong, N. Ewin, R. Richardson, D. A. Howey, and M. D. McCulloch, "The value of a clutch mechanism in electric vehicles," in *2013 World Electric Vehicle Symposium and Exhibition (EVS27)*, pp. 1–11, Nov. 2013.

[10] P. Dolcini, *Contribution to the clutch comfort*. Doctoral Thesis, Departement Automatique / Robotique, Institut National Polytechnique de Grenoble - INPG, France, May 2007. [Online] Available: https://theses.hal.science/tel-00172303.

[11] T. A. Johansen and T. I. Fossen, "Control allocation—A survey," *Automatica*, vol. 49, pp. 1087–1103, May 2013.

[12] H. Fujimoto and S. Harada, "Model-Based Range Extension Control System for Electric Vehicles With Front and Rear Driving–Braking Force Distributions," *IEEE Transactions on Industrial Electronics*, vol. 62, pp. 3245–3254, May 2015.

[13] M. Montazeri-Gh, Z. Pourbafarani, and M. Mahmoodi-k, "Comparative study of different types of PHEV optimal control strategies in real-world conditions," *Proceedings of the Institution of Mechanical Engineers, Part D: Journal of Automobile Engineering*, vol. 232, pp. 1597–1610, Oct. 2018.

[14] C. Xu, X. Guo, and Q. Xun, "Loss Minimization Based Energy Management for a Dual Motor Electric Vehicle," in *2022 IEEE Transportation Electrification Conference and Expo, Asia-Pacific (ITEC Asia-Pacific)*, pp. 1–6, Oct. 2022.

[15] B. Lenzo, G. De Filippis, A. M. Dizqah, A. Sorniotti, P. Gruber, S. Fallah, and W. De Nijs, "Torque Distribution Strategies for Energy-Efficient Electric Vehicles With Multiple Drivetrains," *Journal of Dynamic Systems, Measurement, and Control*, vol. 139, Aug. 2017.

[16] A. Pennycott, L. D. Novellis, P. Gruber, A. Sorniotti, and T. Goggia, "Enhancing the Energy Efficiency of Fully Electric Vehicles via the Minimization of Motor Power Losses," in *2013 IEEE International Conference on Systems, Man, and Cybernetics*, pp. 4167–4172, Oct. 2013.

[17] L. Liberti, "Undecidability and hardness in mixed-integer nonlinear programming," *RAIRO - Operations Research, Publisher: EDP Sciences*, vol. 53, pp. 81–109, Jan. 2019.

[18] D. Zhu, E. Pritchard, S. R. Dadam, V. Kumar, and Y. Xu, "Optimization of rule-based energy management strategies for hybrid vehicles using dynamic programming," *Combustion Engines*, vol. 184, pp. 3–10, Mar. 2021.

[19] N. Murgovski, L. Johannesson, J. Sjöberg, and B. Egardt, "Component sizing of a plug-in hybrid electric powertrain via convex optimization," *Mechatronics*, vol. 22, pp. 106–120, Feb. 2012.

[20] P. Belotti, C. Kirches, S. Leyffer, J. Linderoth, J. Luedtke, and A. Mahajan, "Mixed-integer nonlinear optimization*†," *Acta Numerica*, vol. 22, pp. 1–131, May 2013.

[21] A. Ganesan, S. Gros, and N. Murgovski, "Numerical Strategies for Mixed-Integer Optimization of Power-Split and Gear Selection in Hybrid Electric Vehicles," *IEEE Transactions on Intelligent Transportation Systems*, vol. 24, pp. 3194–3210, Mar. 2023.

[22] L. Lu, C. M. Anderson-Cook, and T. J. Robinson, "Optimization of Designed Experiments Based on Multiple Criteria Utilizing a Pareto Frontier," *Technometrics*, vol. 53, pp. 353–365, Nov. 2011.